AGU PUBLICATIONS

JGR

Journal of Geophysical Research: Atmospheres

RESEARCH ARTICLE
10.1002/2017JD026482

Hemispheric differences in the annual cycle of tropical lower stratosphere transport and tracers

O. V. Tweedy[1], D. W. Waugh[1], R. S. Stolarski[1,2], L. D. Oman[2], W. J Randel[3], and M. Abalos[3]

[1]Department of Earth and Planetary Sciences, JHU, Baltimore, Maryland, USA, [2]NASA Goddard Flight Center, Greenbelt, Maryland, USA, [3]National Center for Atmospheric Research, Boulder, Colorado, USA

Key Points:
- The majority of the CCMs produce the observed feature of a larger annual cycle in the NT than ST ozone and other chemical tracers
- Seasonality in vertical advection drives the seasonality in ST ozone while seasonality of horizontal mixing determines the NT seasonal cycle

Correspondence to:
O. V. Tweedy,
otweedy1@jhu.edu

Citation:
Tweedy, O. V., D. W. Waugh, R. S. Stolarski, L. D. Oman, W. J Randel, and M. Abalos (2017), Hemispheric differences in the annual cycle of tropical lower stratosphere transport and tracers, *J. Geophys. Res. Atmos.*, *122*, 7183–7199, doi:10.1002/2017JD026482.

Received 23 JAN 2017
Accepted 16 JUN 2017
Accepted article online 19 JUN 2017
Published online 8 JUL 2017

Abstract Transport in the tropical lower stratosphere plays a major role in determining the composition of the entire stratosphere. Previous studies that quantified the relative role of transport processes have generally assumed well-mixed tropics and focused on tropical-wide average characteristics. However, it has recently been shown that there is a hemispheric difference in the annual cycle of tropical lower stratosphere ozone and other tracers, with a larger amplitude in the northern tropics (NT) than in the southern tropics (ST). In this study, we examined the ability of chemistry climate models (CCMs) to reproduce the hemispheric differences in ozone (O_3) and other tracers (i.e., hydrochloric acid, or HCl and nitrous oxide, or N_2O), and then use the CCMs to examine the cause of these differences. Examination of CCM simulations from the CCMVal-2 project shows that the majority of the CCMs produce the observed feature of a larger annual cycle in the NT than ST O_3 and other tracers. However, only around a third of the models produce an ozone annual cycle similar to that observed. Transformed Eulerian Mean analysis of two of the CCMs shows that seasonality in vertical advection drives the seasonality in ST O_3 and N_2O while seasonality of horizontal mixing drives the seasonality in NT O_3 and N_2O, with a large increase in horizontal mixing during northern summer (associated with the Asian monsoon). Thus, latitudinal and longitudinal variations within the tropics have to be considered to fully understand the balance between transport processes in tropical lower stratosphere.

1. Introduction

Transport in the tropical lower stratosphere plays a key role in determining the stratospheric spatial and temporal distribution of ozone (O_3), water vapor, aerosols, and other trace constituents, and the coupling between the stratosphere and climate [*Fueglistaler et al.*, 2009; *Riese et al.*, 2012]. It is therefore important to understand and quantify this transport, and how it may change in the future.

Transport of chemical tracers is often decomposed into vertical and quasi-horizontal components. The vertical transport in the tropics is dominated by the large-scale ascent by the Brewer-Dobson circulation while the quasi-horizontal transport (we will refer to it as simply horizontal transport) is associated with the eddy mixing. The effect of these two transport processes on chemical constituents whose dynamical time scales are longer than time scales for chemical sources and sinks (long-lived tracers) is to increase and decrease latitudinal gradients in the case of vertical and horizontal transport, respectively [e.g., *Andrews et al.*, 1987, chapter 9].

Temporal variability of O_3 and other long-lived tracers in the tropical lower stratosphere is strongly influenced by the transport processes described above as well as by the photochemical production and loss. However, the relative importance of different processes in the tropics remains uncertain. *Randel et al.* [2007] explained the large seasonal cycle in the lower stratospheric ozone as a response to seasonal changes in upwelling, assuming the seasonality of eddy transport is small. However, effective diffusivity calculations of *Haynes and Shuckburgh* [2000] showed mixing into the tropical lower stratosphere, and a number of more recent studies have shown that horizontal mixing within the extratropics plays an important role [e.g., *Konopka et al.*, 2009, 2010; *Abalos et al.*, 2012, 2013a, 2013b; *Ploeger et al.*, 2012]. For example, *Konopka et al.* [2009] reported that mixing by eddies is responsible for about 40% of the observed O_3 mixing ratios during boreal summer in the lower stratosphere, while *Abalos et al.* [2013b] demonstrated the dominant role of horizontal transport near

©2017. American Geophysical Union. All Rights Reserved.

the tropical tropopause and increasing role of vertical advection above 70 hPa. Horizontal mixing is primarily driven by the large anticyclonic circulations above Asia and North America in the upper troposphere and lower stratosphere (Asian and North American monsoons). The studies described above emphasized the important role of horizontal and vertical transport in the tropical lower stratosphere from different perspectives [*Abalos et al.*, 2013a]; however, the exact balance between upwelling by the residual circulation and eddy mixing (and how this balance varies with altitude) remains a topic of debate.

An additional complication for understanding the annual cycle in O_3 is the feedback between ozone and upwelling by the residual circulation ($\bar{w}^*$) [*Andrews et al.*, 1987]. Changes in O_3 lead to changes in heating rates that impact the upwelling and then O_3 [*Ming et al.*, 2016b]. Furthermore, changes in ozone heating rates would impact $\bar{w}^*$ indirectly through changes in wave-induced forcing [*Ming et al.*, 2016a]. This is, however, not an issue for nitrous oxide (N_2O) and other long-lived tracers which do not have a significant radiative impact in the tropical lower stratosphere.

A further uncertainty comes from the fact that the above studies have focused primarily on the variations in the tropical-wide average (20°N–20°S) of tracers, i.e., have considered "well-mixed" tropics. Recently, *Stolarski et al.* [2014] showed significant differences in the observed seasonality of O_3 and other tracers between the northern and southern tropics (NT and ST, respectively). In particular, they showed that the amplitude of the seasonal cycle in O_3 in the NT is stronger than that in the ST, and that the maximum in O_3 mixing ratio in the NT occurs in July–August while in the ST it occurs 1–2 months later. Further, they concluded from an analysis of $\bar{w}^*$ that seasonal variations in upwelling alone could not explain the hemispheric contrast in annual cycle of tracers, and there must be other processes that affect the seasonality of the tracers in the tropical lower stratosphere. In this study, we further examine the NT-ST difference in annual cycle of tracers (O_3, N_2O, and HCl) using Chemistry-Climate Model (CCM) simulations. We first evaluate the ability of the suite of CCMs from the Chemistry-Climate Model Validation activity phase 2 (CCMVal-2) [*Eyring et al.*, 2008] to reproduce the observed tracer annual cycles. We then examine the relative role of different transport processes and chemical production and loss in producing the O_3 and N_2O annual cycles in the ST and NT. This analysis includes an examination of the differences in O_3/N_2O and $\bar{w}^*$ among the CCMVal-2 simulations, as well as a more detailed Transformed Eulerian Mean (TEM) analysis of two of the CCMs within CCMVal-2.

The observations and models used and method of analysis are described in the next section. In section 3 we evaluate the ability of the CCMVal-2 models to reproduce the observed tracer annual cycles, while in section 4 we perform a more detailed analysis of two of the CCMs.

2. Models, Observational Data, and Methods

2.1. Chemistry Climate Models

We examine simulations from CCMs that participated in the second CCM Validation (CCMVal-2) project [*Eyring et al.*, 2008]. CCMVal-2 was an international project, organized under the auspices of WCRPs (World Climate Research Programme) SPARC (Stratosphere Processes and their Role in Climate) project [*SPARC CCMVal*, 2010], designed to compare and evaluate stratospheric CCMs. The CCMs considered here are listed in Table 1. All of these models include stratospheric chemistry that is radiatively coupled to the dynamics, i.e., the distributions of radiatively active gasses (e.g., CO_2, H_2O, N_2O, CFCs, and O_3) influence the radiative heating rates and thus dynamics. We use the "historical" REF-B1 simulation that covers the period 1960–2006. These simulations include natural and anthropogenic forcings based on observed changes in the abundance of trace gases and were designed to provide the best possible representation of the stratospheric climate and variability over this period. A more extensive description of these models and simulations is provided in *Morgenstern et al.* [2010] and references in Table 1.

We first examine the ability of all CCMs listed in Table 1 to reproduce the observed hemispheric differences in annual cycles of tropical ozone and other trace gases and then focus in more detail on simulations from the Goddard Earth Observing System Chemistry Climate Model (GEOSCCM) and the Whole-Atmosphere Community Climate Model (WACCM). We have access to fields not in the CCMVal-2 data archive from these two models that enable a more detailed analysis of the transport in the tropical lower stratosphere.

GEOSCCM couples the Goddard Earth Observing System (GEOS) general circulation model with a comprehensive stratospheric chemistry module. The GEOSCCM simulations in CCMVal-2 used version 5 of GEOS (GEOS-5), described in *Pawson et al.* [2008]. The GEOSCCM simulations analyzed have horizontal resolution of 2° latitude by 2.5° longitude and include 72 vertical levels from the surface up to 0.01 hPa (80 km). GEOSCCM performed

Table 1. CCMVal-2 Models With References and Half Peak-to-Peak Annual Cycle Amplitude in O_3 and w[a]

Number	Models	Reference	ST O3 (%)	NT O3 (%)	ST w* (mm/s)	NT w* (mm/s)
1	AMTRAC3	*Austin and Wilson* [2006]	20.4	30.4	N/A	N/A
2	CAM3.5	*Lamarque et al.* [2008]	16.6	39.06	0.181	0.164
3	CCSRNIES	*Akiyoshi et al.* [2009]	30.0	18.4	0.278	0.113
4	CMAM	*Scinocca et al.* [2008]	27.6	29.0	0.367	0.223
5	CNRM	*Teyssédre et al.* [2007] and *Déqué* [2007]	27.7	42.5	0.387	0.500
6	E39CA	*Garny et al.* [2009]	21.4	19.5	0.241	0.138
7	EMAC	*Jöckel et al.* [2006]	24.4	29.0	0.195	0.217
8	GEOSCCM	*Pawson et al.* [2008]	15.8	37.0	0.113	0.086
9	LMDZrepro	*Jourdain et al.* [2008]	22.9	36.9	0.157	0.125
10	MRI	*Shibata and Deushi* [2008]	23.4	15.9	0.204	0.104
11	Niwa-SOCOL	*Schraner et al.* [2008]	10.6	16.1	0.270	0.238
12	SOCOL	*Schraner et al.* [2008]	8.7	14.7	0.233	0.136
13	ULAQ	*Pitari et al.* [2002]	39.7	14.0	0.476	0.454
14	UMETRAC	*Austin and Butchart* [2003]	19.3	26.0	N/A	N/A
15	UMSLIMCAT	*Tian and Chipperfield* [2005]	18.9	25.0	N/A	N/A
16	UMUKCA-METO	*Morgenstern et al.* [2009, 2010]	15.9	16.8	N/A	N/A
17	UMUKCA-UCAM	*Morgenstern et al.* [2009, 2010]	10.7	22.0	0.102	0.057
18	WACCM	*Garcia et al.* [2007]	24.1	44.7	0.174	0.157

[a]The models are listed in numerical order as they appear in Figure 3.

well in evaluations of both chemical- and transport-related processes [*SPARC CCMVal*, 2010; *Strahan et al.*, 2011; *Douglass et al.*, 2012]. The required output for a full Transformed Eulerian Mean (TEM) budget analysis was not archived from the CCMVal-2 simulations but is available for simulations from an updated version of GEOSCCM, described in *Oman and Douglass* [2014]. The annual cycle of ozone and other tracers in the tropical lower stratosphere is very similar between the two GEOSCCM simulations.

WACCM is the atmospheric component of the coupled climate system model Community Earth System Model, Version 1 and is described in *Garcia et al.* [2007]. It has horizontal resolution of 2.5° latitude and 1.9° longitude and extends vertically from the ground up to the lower thermosphere (180 km) with 66 vertical levels. Vertical resolution in the upper troposphere and lower stratosphere is 1.1–1.4 km. As with GEOSCCM, the required fields for the TEM analysis were not archived for the CCMVal-2 REF-B1 historical simulation but are available from a later WACCM simulation. The later simulation is described in *Abalos et al.* [2013b], where it is shown that the simulated annual cycle in ozone and temperature agrees well with satellite observations. As with the GEOSCCM simulations, there is good agreement in the ozone distributions between the two WACCM simulations considered here.

2.2. Observational Data

The ability of CCMs to realistically represent ozone and its seasonality in the tropical lower stratosphere is evaluated against measurements from several satellite instruments. *Stolarski et al.* [2014] examined the seasonality of tropical lower stratospheric ozone from the Stratospheric Aerosol and Gas Experiment II (SAGE II) [*Wang et al.*, 2002] and version 3 of the Aura Microwave Limb Sounder (MLS-v3) [*Livesey et al.*, 2008] instruments. We consider these data sets together with a new version of MLS (MLS-v4), which incorporates some modifications that improve ozone vertical profiles [*Livesey et al.*, 2015], and measurements from the Ozone Mapping and Profile Suite (OMPS) on board NASA/NOAA Suomi-NPP satellite [*Kramarova et al.*, 2014].

SAGE II data are available from 1984 to 2005, MLS from September 2004 to present, and OMPS from 2012 to present. We use MLS and OMPS data up to 2015 in our analysis. The MLS and OMPS data have sufficient horizontal and temporal coverage to enable examination of the ozone annual cycle for each year. MLS has a vertical resolution around 3 km, whereas OMPS has higher vertical resolution of around 1.5–2 km. SAGE II also has higher vertical resolution than MLS (~1 km), but has sparser spatial and temporal coverage, and the long (21 year) data set is needed to create a climatology with a good horizontal and temporal coverage.

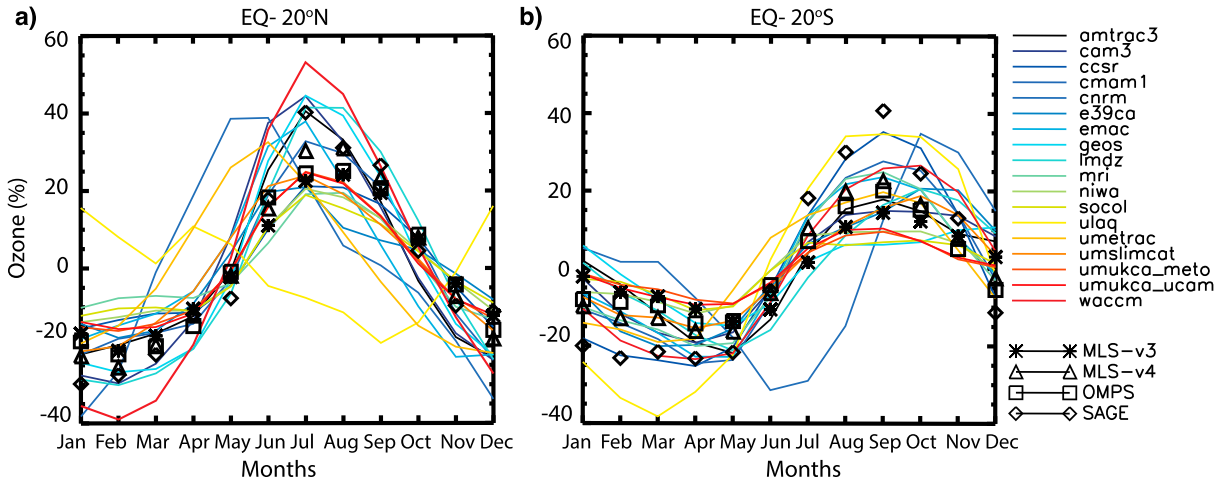

Figure 1. Seasonal evolution of lower stratospheric (~80 hPa) ozone deviations averaged over (a) NT and (b) ST, from observations (black symbols) and CCMVal-2 models (colored lines). Values are shown as percent difference of climatological monthly averaged ozone from its climatological annual mean.

The observational data sets described above are publicly available. MLS data are available from the NASA Goddard Space Flight Center Earth Sciences Data and Information Services Center. OMPS satellite ozone data have been obtained from the NASA Goddard Space Flight Center website (https://jointmission.gsfc.nasa.gov/omps.html), and SAGE II ozone data have been obtained from the Langley Data Center (https://eosweb.larc.nasa.gov).

2.3. Calculations of the Climatological Annual Cycle

We focus on the climatological annual cycle of tracers and $\bar{w}^*$, i.e., we examine seasonal changes in the climatological monthly-mean values. The climatological means from the CCMs are formed by averaging output from 1990 to 2005, while the periods used for the observations vary among data sets (see above). The amplitudes of the tracers and $\bar{w}^*$ annual cycle are calculated as half the difference between the maximum and minimum in monthly climatologies. This yields results similar to fitting annual sines and cosines to the full monthly-mean ozone time series (as done in *Stolarski et al.* [2014]).

The results of our analysis are not sensitive to the time interval used to create the climatology. Ozone annual cycle amplitudes computed using three different time intervals (1960–2005, 1980–2005, and 1990–2005) give very similar results (differences in annual amplitude are less than 3%, not shown). While there is some interannual variability in the details of stratospheric ozone and $\bar{w}^*$ seasonality, our results are representative of typical seasonal cycle variability within the considered time period.

3. Evaluation of CCMVal-2 Models

We first evaluate the ability of the CCMs to reproduce the observed annual cycle of tropical ozone. Figure 1 shows the seasonal evolution of climatological monthly-mean O_3 at 80 hPa from the CCMs (colored curves) and satellite observations (black symbols), for averages over the (a) northern tropics (NT; 0–20°N) and (b) southern tropics (ST; 0–20°S). The observations show, as discussed in *Stolarski et al.* [2014], a larger amplitude in the NT than in the ST, and a 1–2 month lag in the timing of the peak between the ST and NT. There are some differences among the data sets (see further discussion below), but these differences are much smaller than the spread in the simulated ozone annual cycle among the models. While some models produce an annual cycle with similar amplitude and phase, there are models with amplitude much smaller or much larger than observed, and some models have the incorrect phase.

To examine the differences among the models, and among the data sets, we show the latitude-pressure variation in the amplitude of the ozone annual cycle in Figure 2. As discussed above, the observational data sets (top row) all show larger amplitude in northern than southern tropics in the lower stratosphere. They also all show that this NT-ST difference goes away in the middle and upper stratosphere. There are, however, differences among the data in the vertical variations in the lower stratosphere, including where the maximum amplitude occurs (with SAGE II showing the peak at a higher altitude than MLS or OMPS) and whether there is

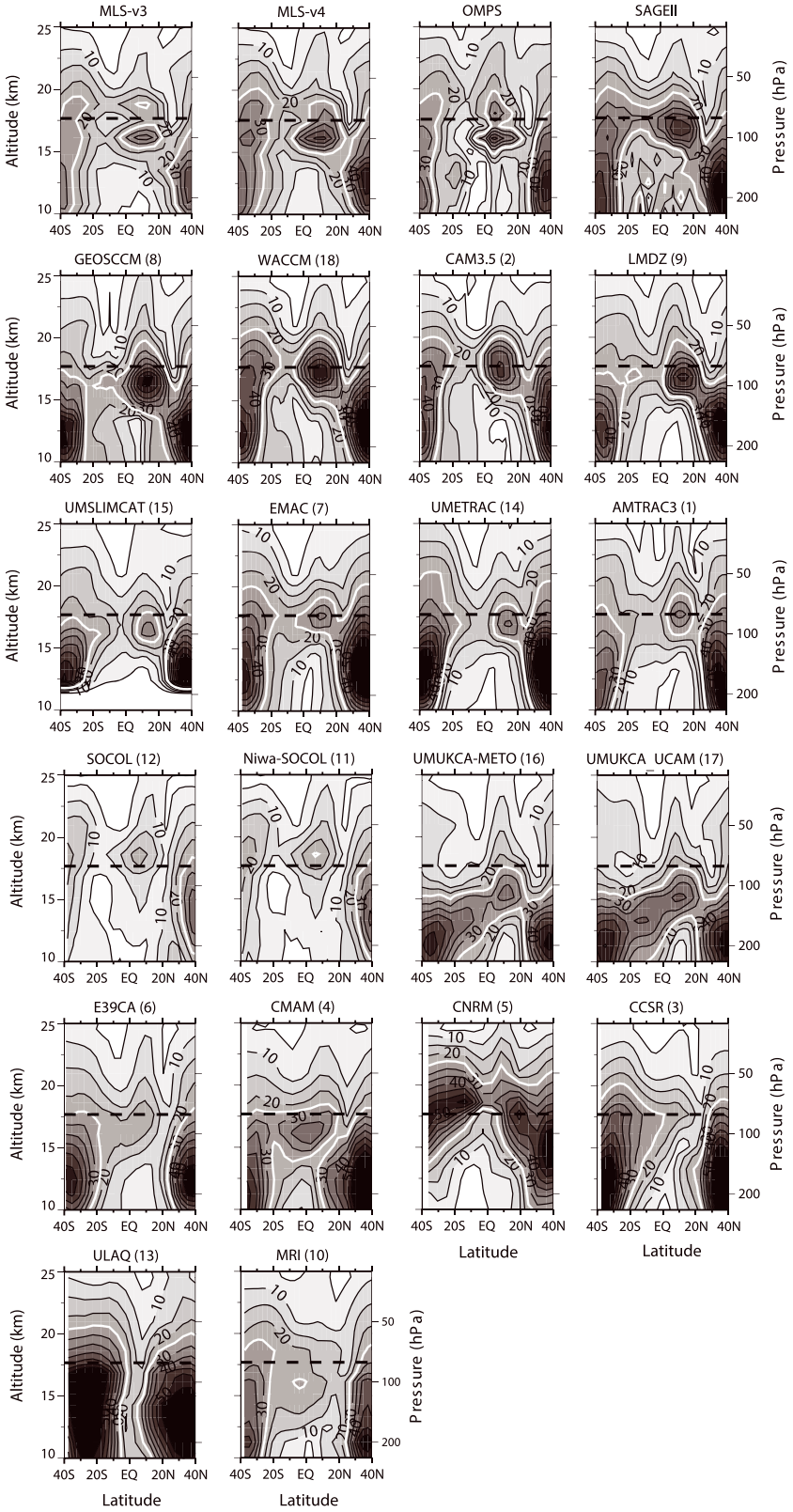

Figure 2. Latitude-altitude dependence of the magnitude of the annual cycle in ozone, in percent of the annual-mean value, from 4 observational data sets (MLS-v3, MLS-v4, OMPS, and SAGE II) and 18 CCMVal-2 models (see Table 1). Contour interval is every 5% with thick white contour corresponding to 25%. The 80 hPa vertical level is indicated by dashed lines.

a two-peak structure in the vertical. As discussed in *Stolarski et al.* [2014], SAGE II measurements show only a single peak in the annual cycle amplitude in the lower stratosphere, while MLS (-v3) shows a double peak with local maximum at 100 and 68 hPa. This two-peak structure is not found in the ozonesondes (not shown) and in the newer version of MLS (-v4) but occurs in OMPS. The cause of these differences between the different observational data sets is unknown and is the subject of ongoing research.

Consistent with the observations, the majority of the CCMs show a larger amplitude in the northern tropics (NT) than in the southern tropics (ST). This suggests that these CCMs include the key processes (transport and chemical production and loss) that cause the hemispheric differences in tropical ozone seasonality. However, none of the models produce a double peak structure as found in MLS-v3 and OMPS. Also, there are differences in the magnitude of the peak and its location among the CCMs, indicating quantitative differences in the transport among the models. Furthermore, there are several CCMs that do not show a significant hemispheric difference in the annual amplitude (CMAM, CNRM, and 39CA) or even show a larger amplitude in the ST than the NT (ULAQ, CCSR, and MRI), suggesting some problems in the representation of this aspect of transport in the tropical lower stratosphere.

To quantify the differences among models, we calculate the amplitude of the annual cycle of 80 hPa ozone averaged over the NT and ST. The 80 hPa vertical level is highlighted as dashed black horizontal line in Figure 2. Figure 3a shows the relationship between the NT-averaged and ST-averaged amplitude for the CCMs (black diamonds) and for the observations (blue stars). The amplitudes at 80 hPa for each CCM are also listed in Table 1. As discussed above, the majority of the CCMs reproduce the observed feature of larger amplitude in the NT than the ST (i.e., the symbols for the majority of the models lie above the 1-1 line in Figure 3a). However, for some models the NT and ST amplitudes have similar values or the ST amplitude is larger than the NT amplitude. There is also a large spread in the amplitude of the ST and NT annual cycles among the models. Some of the spread is due to the variations in altitude of the peak in annual cycle amplitude. For example, the NT peak in ozone amplitude from UMUKCA-METO and UMUKCA-UCAM is located below 80 hPa reaching a maximum near 100 hPa (see Figure 2). Note that given the differences between the annual cycle in different observational data sets we are limited on how precise we can be in determining the reality of the simulated annual cycle. However, even with this uncertainty there are models that are well outside the observational estimates.

A similar analysis of the NT-averaged and ST-averaged amplitude of annual cycle in other long-lived tracers (e.g., N_2O, HCl, and mean age) shows very similar results, with a wide spread in amplitudes among the CCMs and CCMs with larger (smaller) O_3 amplitude in the NT than ST also have a larger (smaller) NT amplitude for the other tracers (not shown). This suggests that the NT-ST contrast in annual amplitude is driven by transport and not chemistry.

What could be causing the differences in the annual cycle in NT and ST ozone among the CCMs? One potential cause is differences in the simulated annual cycle of tropical vertical residual circulation ($\bar{w}^*$). Figure 3b shows the relationship between amplitude of NT and ST $\bar{w}^*$ at 100 hPa for the CCMs (where $\bar{w}^*$ is available) and several meteorological reanalyses. Most models show the same qualitative differences between the amplitude of ST and NT $\bar{w}^*$ as in the reanalyses (i.e., larger annual cycle in the ST than in the NT), but with some large quantitative differences among the models. However, there are two models ((5) CNRM and (13) ULAQ) with $\bar{w}^*$ amplitudes in the ST and NT considerably larger than in other models, indicating serious problems with simulated $\bar{w}^*$. Furthermore, the differences in $\bar{w}^*$ among CCMs may only explain some portion of the spread in the O_3 annual cycle amplitude, and they do not explain all the differences. For example, models 16 and 17 (UMUKCA-METO and UMUKCA-UCAM) have the smallest amplitudes of $\bar{w}^*$ annual cycle, but the O_3 amplitudes are comparable or larger than observed. This indicates that differences in the $\bar{w}^*$ annual cycle are not the only differences in the transport among the models. The fact that other processes are playing a role can also be seen, as discussed in *Stolarski et al.* [2014], by comparing the relative NT-ST amplitudes of $\bar{w}^*$ and O_3: A larger annual cycle of $\bar{w}^*$ in the ST than the NT will, if no other hemispheric differences, produce a larger ST cycle in ozone. This is not observed or simulated in most models, indicating other processes play a role.

To explore this further we examine the relationship between the amplitude of the annual cycle in O_3 and vertical transport by the residual circulation. The local change in tracer concentration due to transport processes and chemical sources and sinks can be quantified by the zonal mean continuity equation [*Andrews et al.*, 1987, equation (9.4.13)]:

$$\bar{\chi}_t = -\bar{v}^* \bar{\chi}_y - \bar{w}^* \bar{\chi}_z + e^{z/H} \nabla \cdot \mathbf{M} + P - L \quad (1)$$

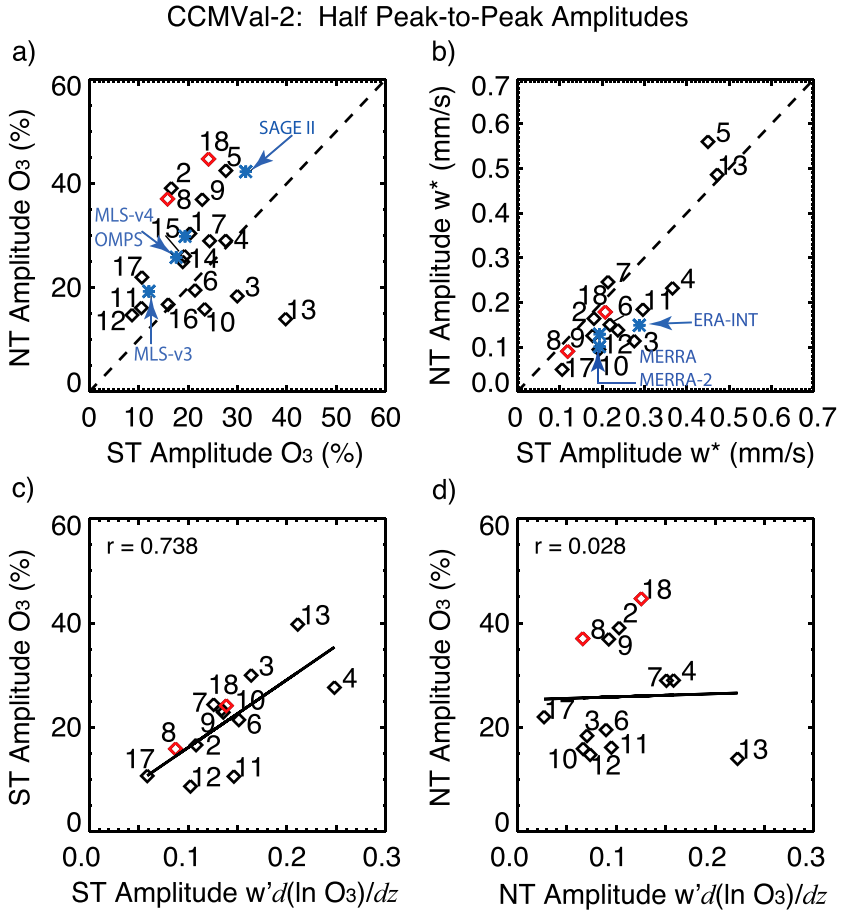

Figure 3. (a) The magnitude of ozone seasonality at 80 hPa averaged over the NT (0–20°N) versus the magnitude averaged over the ST (0–20°S) for 18 models (black diamonds) from the CCMVal-2 intercomparison project. The symbols in red show model simulations from (8) GEOSCCM and (18) WACCM. The blue stars correspond to four data sources: MLS-v3, MLS-v4, OMPS, and SAGE II. (b) The same as in Figure 3a except for magnitude of the annual cycle in $\bar{w}^*$ at 100 hPa for 14 models from the CCMVal-2 intercomparison project (in black) with blue stars representing three reanalysis products (Modern-Era Retrospective analysis for Research and Applications (MERRA), MERRA-2, and European Centre for Medium-Range Weather Forecasts Re-Analysis (ERA-Interim)). (c, d) Relationship between ozone amplitude and vertical transport ($w' \frac{\partial(\ln \overline{O_3})}{\partial z}$) for the CCMs, for ST (Figure 3c) and NT (Figure 3d). The linear regression between ozone and vertical advection is shown in Figures 3c and 3d, with Pearson linear correlation coefficient (r) in the left right corner.

where $(\bar{v}^*,\bar{w}^*)$ is the residual circulation, $P - L$ is the chemical production minus loss rate, and M is the eddy transport vector. The first two terms on the right-hand side correspond to horizontal and vertical advection, while the third term is the combined horizontal and vertical eddy transport term. The components of the divergence of eddy transport vector are as follows:

$$M_y = -e^{z/H}\left(\overline{v'\chi'} - \frac{\overline{v'T'}}{S}\overline{\chi}_z\right) \tag{2}$$

$$M_z = -e^{z/H}\left(\overline{w'\chi'} - \frac{\overline{v'T'}}{S}\overline{\chi}_y\right) \tag{3}$$

Assuming the annual cycle in tracers is determined only by vertical advection (i.e., seasonality of horizontal advection, $P - L$, and eddy transport are small), *Randel et al.* [2007] showed the relationship between annual variations in tracer and vertical transport in the tropics:

$$i\sigma\frac{\chi'}{\langle\bar{\chi}\rangle} = w'\frac{\partial(\ln\bar{\chi})}{\partial z} \tag{4}$$

where $\frac{\chi'}{\langle\bar{\chi}\rangle}$ is the fractional annual amplitude of tracer (i.e., annual amplitude divided by annual-mean value), w' is annual amplitude of upwelling by the residual circulation, and $\sigma = 2\pi/(365\ \text{days})$. Figures 3c and 3d show the relationship between fractional annual amplitude of ozone and $w'\frac{\partial(\ln\bar{\chi})}{\partial z}$ for ST (Figures 3c) and (Figures 3d) NT averages. If the annual cycle in vertical transport is a major driver in the annual cycle of ozone, then we may expect a linear relationship between these two terms.

Figure 3c shows that this is generally true for the ST amplitude, as CCMs with larger annual cycles in ST vertical transport also have a larger O_3 amplitude. The steep slope of the regression line and large linear Pearson correlation coefficient ($r = 0.73$) strongly suggest that variations in the amplitude of the ST annual cycle in vertical transport explain variations in the ST ozone annual cycle. This is not the case for the NT annual cycles, where there is no relationship ($r = 0.03$ and nearly zero slope of the linear fit) between the amplitude of ozone and $\bar{w}^*$ (Figure 3d). This is consistent with the conclusions from *Stolarski et al.* [2014] that upwelling is not the determining factor in the NT ozone annual cycle and that other processes (such as horizontal mixing and/or chemistry) play a larger role.

Previous studies have also evaluated the transport in suite CCMVal-2 models, and it is interesting to compare their evaluations with our analysis of the CCMs ability to simulate the NT and ST annual cycles. In particular, *Strahan et al.* [2011] evaluated the CCMs considered here based on the model's ability to correctly represent ascent and horizontal mixing based on N_2O and mean age and classified the CCMs into those with the "most realistic stratospheric transport" (CAM3.5, CMAM, GEOSCCM, UMSLIMCAT, and WACCM), "slow ascent or too much mixing" (LMDZ, MRI, ULAQ, UMUKCA-METO, and UMUKCA-UCAM), or "too fast transport" (AMTRAC3, UMETRAC, CNRM, NIWA-SOCOL, and SOCOL). Their results also showed that the five models with the best representation of circulation and mixing show closer agreement with MLS O_3 than most models, and the spread among them is smaller. The six models—AMTRAC3, CCSRNIES, LMDZ, NiwaSOCOL, SOCOL, and UMETRAC—with less serious transport deficiencies compare well with observations in the tropical lower stratosphere as do the models with realistic transport, while models with significant transport problems (such as ULAQ, CNRM, and MRI) show large deviations in simulated tropical ozone. Our multimodel analysis shows that four out of the five models with the most realistic transport also do well in reproducing the NT-ST differences in ozone annual cycle (CMAM is the exception as it has a similar amplitude in the NT and ST), while the CCMs with too slow or fast transport or too much mixing generally also have unrealistic aspects of their tropical lower stratospheric ozone annual cycle. AMTRAC, LMDZ, and UMETRAC (models with less serious problems) are exceptions, as the amplitudes of NT and ST annual cycles in these models are close to observed. It is unclear why CMAM reproduces N_2O and mean age well but not the ST-NT contrast in the ozone annual cycle and why AMTRAC and LMDZ get the ozone annual cycle but not N_2O and mean age. We are limited in our ability to answer these questions because of the lack of required data in the CCMVal archive, e.g., $\bar{w}^*$ is not archived for some models and even fewer models have available outputs to perform detailed TEM or related analysis.

4. Detailed Analysis of GEOSCCM and WACCM

We now use GEOSCCM and WACCM simulations to examine the transport processes and annual cycle of ozone and other tracers in more detail. As described in section 2 we have access to fields that are not in the CCMVal-2 archive from these models.

The analysis above shows that simulations from these two CCMs capture the observed larger amplitude of the seasonal cycle in the lower stratospheric ozone in the NT than in the ST (Figure 2). Latitudinal variations in seasonality of lower stratospheric ozone are also very similar between these two models and observations, as illustrated in Figure 4a (pattern correlation coefficient is above 0.95). There are strong meridional gradients (i.e., contours are close together) in midlatitudes but much weaker gradients (contours further apart) in the tropics. In the southern subtropics, there is only weak seasonality in ozone, with slightly higher values around October. In contrast, there is large seasonality in the northern tropics with a large increase in June to August, where the spreading of the contours indicates transport of high ozone values from the midlatitudes into the tropics. This northern-southern contrast explains the large difference in annual amplitude between the NT and ST. While WACCM and GEOSCCM produce ozone structure similar to that observed, there are differences in the magnitude of the meridional gradients and extent to which high ozone values intrude into the tropics during northern summer.

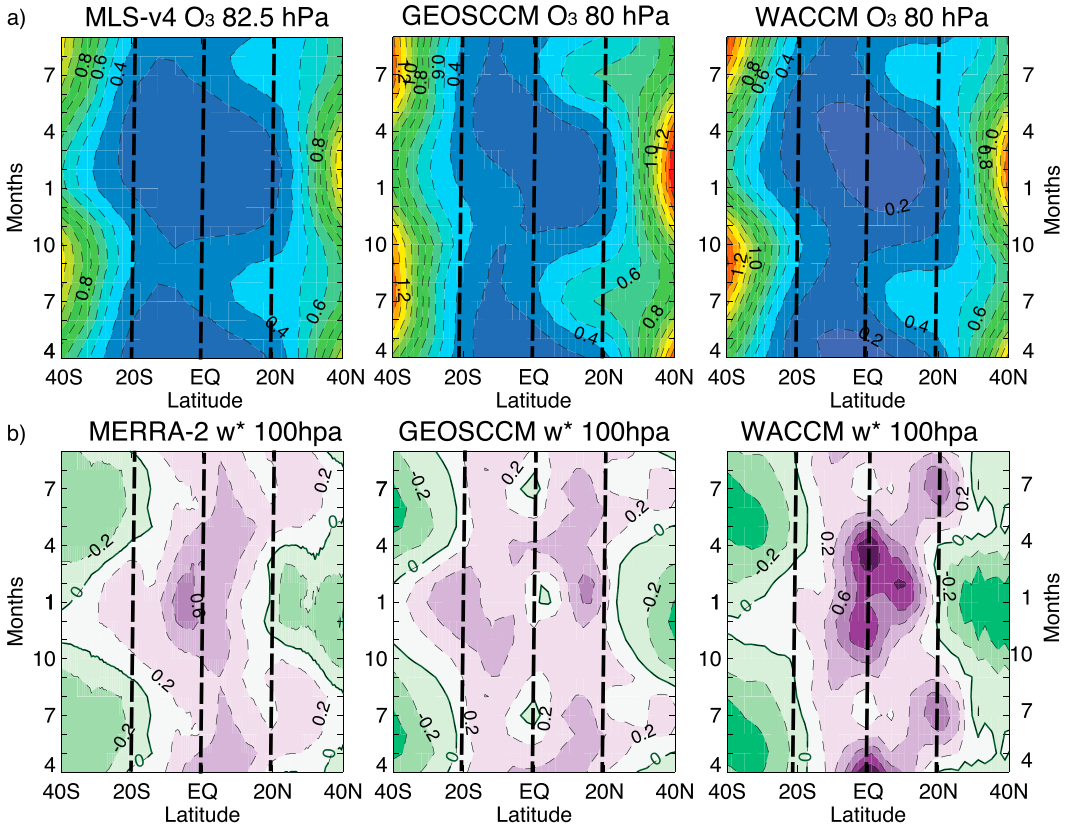

Figure 4. Latitudinal variations of seasonality in (a) ozone and (b) residual vertical velocity, $\bar{w}^*$, in the tropical lower stratosphere in MLS-v4/MERRA-2, WACCM, and GEOSCCM. Ozone is averaged between 80 and 90 hPa (82 hPa for MLS), while $\bar{w}^*$ is shown at 100 hPa. Thick dashed lines indicate the boundaries of the NT and ST. Contour intervals are every 0.1 ppmv for ozone and 0.2 mm/s for $\bar{w}^*$.

The annual cycle of the upwelling at 100 hPa also looks qualitatively similar (pattern correlation coefficient around 0.80) among these two models and reanalysis (MERRA-2), see Figure 4b. As in the reanalysis, both models capture the oscillating behavior of $\bar{w}^*$ between summer hemispheres with seasonal migration of the edge of the tropical upwelling toward the pole in spring and then back toward the equator in autumn. Although $\bar{w}^*$ is larger in WACCM than in GEOSCCM and MERRA-2, there is a good agreement with reanalysis on overall structure of the tropical upwelling in the lower stratosphere.

While we focus mostly on the seasonality of O_3 in the tropical lower stratosphere, other long-lived tracers such as HCl and N_2O also show differences in the annual cycle between the NT and ST [*Stolarski et al.*, 2014]. These NT-ST differences also occur in GEOSCCM and WACCM simulations, see Figure 5. HCl, like O_3, is produced in the stratosphere and its volume mixing ratios increase rapidly with height and poleward from the equator in the lower stratosphere [see *Stolarski et al.*, 2014, Figure 6], and the seasonal cycles in HCl and O_3 are very similar. In particular, for both tracers the amplitude of the annual cycle is larger, and the peak occurs around 2 months earlier in the NT than ST.

There is also a NT-ST difference for the N_2O annual cycle. The magnitude of seasonal changes in N_2O is much smaller than in O_3 and HCl due to smaller vertical and horizontal gradients of N_2O in the lower stratosphere. As N_2O is produced in the troposphere, its spatial gradients are opposite of O_3 and HCl: rather than a summer maximum in NT there is a summer minimum. In GEOSCCM and WACCM the amplitude of the annual cycle in N_2O is larger in the NT than ST (consistent with other tracers), while for MLS the differences between NT and ST amplitudes are small. Figure 5 shows N_2O mixing ratios from an older version of MLS (v3), since N_2O from MLS-v4 shows unrealistically high values at 68 hPa level [*Livesey et al.*, 2015].

The above analysis demonstrates that GEOSCCM and WACCM simulations capture the hemispheric differences of the observed annual cycle phase and amplitude. The amplitudes in the NT are too large compared

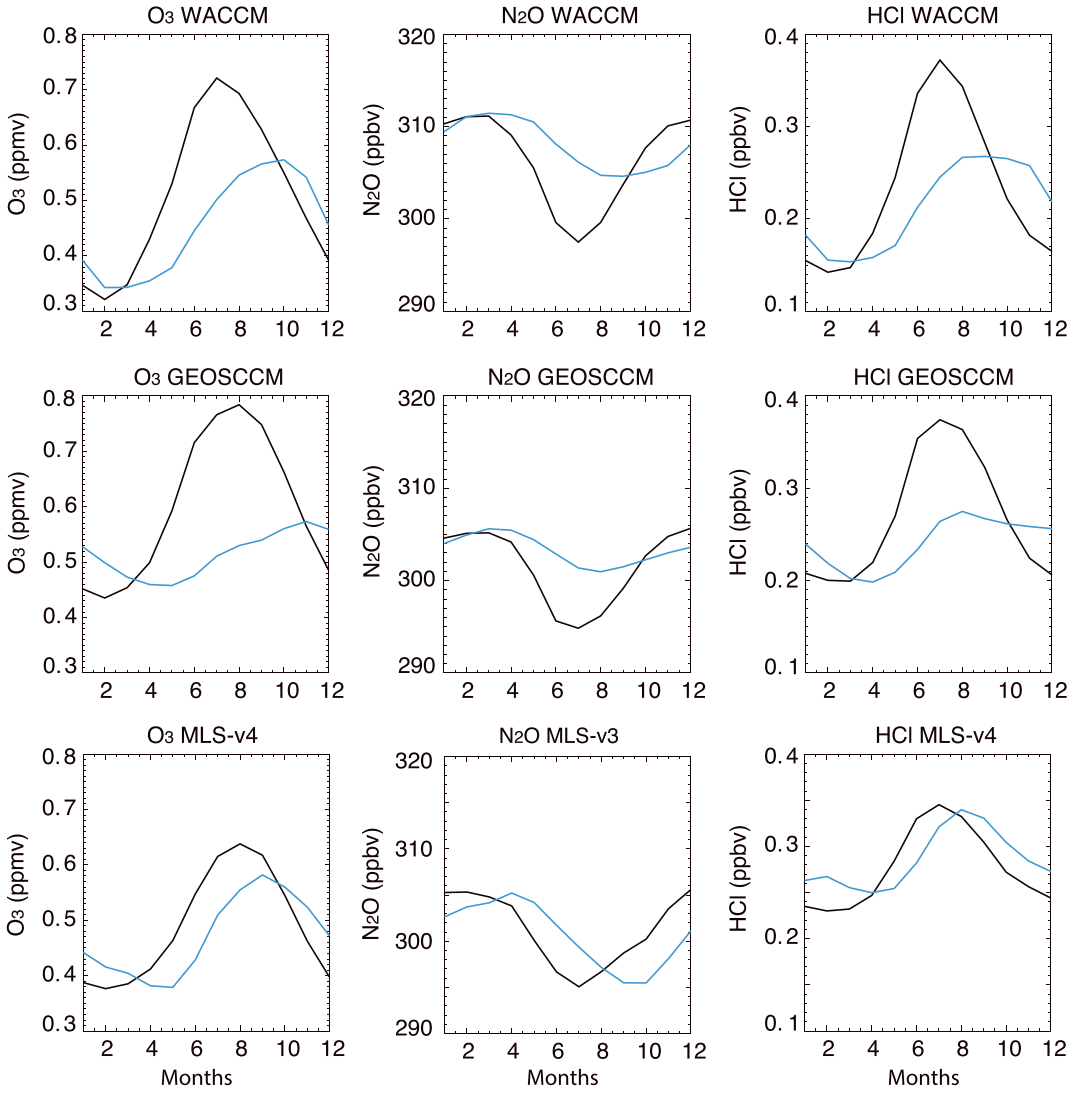

Figure 5. Climatological annual cycle in O_3, N_2O and HCl from (top row) WACCM, (middle row) GEOSCCM, and (bottom) MLS at 70 hPa averaged over northern (black) and southern (blue) tropics. MLS-v3 is used for N_2O because of high N_2O bias in MLS-v4 at this level.

to observations, but as the models capture the observed vertical and horizontal structure of the annual cycle amplitude they can be used to further examine the transport processes producing these structures. We first use the Transformed Eulerian Mean (TEM) formalism to separate the relative importance of transport processes and chemistry on the seasonality of zonal mean O_3 and N_2O and then examine the longitudinal variations in ozone.

4.1. TEM Analysis

The TEM continuity equation for zonal mean tracer concentration (equation (1)) can be used to compute tracer budgets based on the role of transport processes and chemical sources and sinks. Equation (1), therefore, can be rearranged as follows:

$$\bar{\chi}_t = \left[-\bar{v}^*\bar{\chi}_y + e^{z/H}(\cos\phi)^{(-1)}(M_y\cos\phi)_y\right] + \left[-\bar{w}^*\bar{\chi}_z + e^{z/H}(M_z)_z\right] + P - L \tag{5}$$

to separate horizontal (terms in the first bracket) and vertical (terms in the second bracket) transport contributions to tracer tendency.

A complete TEM budget analysis based on observations is not possible as the eddy components cannot be calculated from available observations, but all terms can be calculated from model output. *Abalos et al.* [2013b]

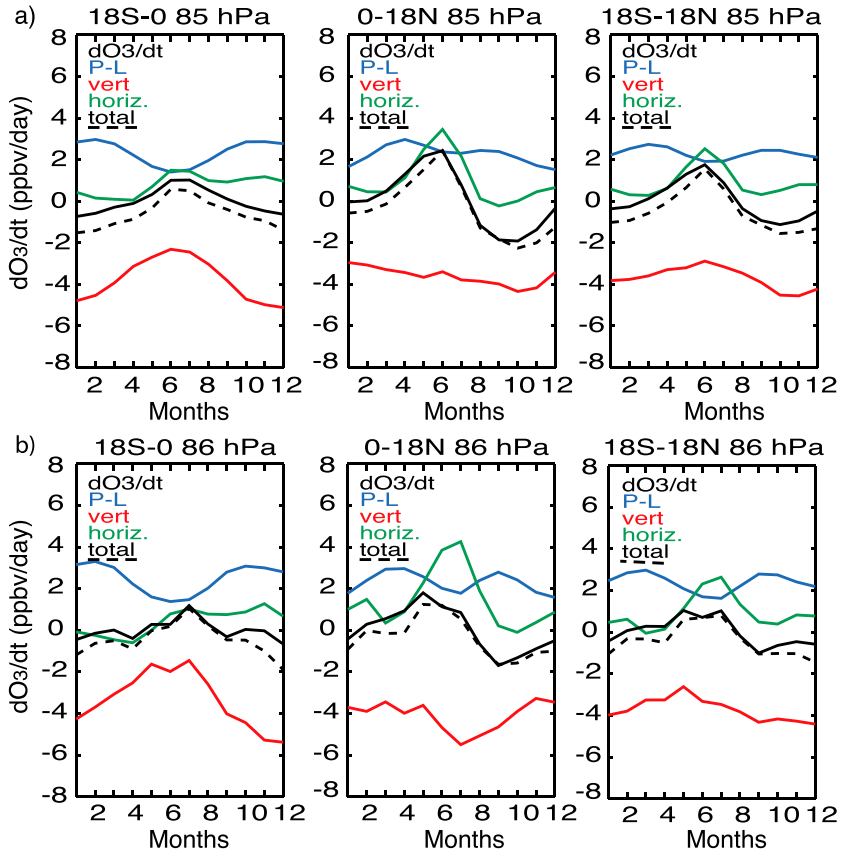

Figure 6. Mean seasonal cycles (monthly means) of terms in the ozone TEM continuity equation at 85 hPa in (a) GEOSCCM and at 86 hPa in (b) WACCM averaged over (left to right) EQ-18°S, EQ-18°N, and 18°S–18°N. Black solid line shows ozone tendency, computed directly from monthly mean zonal mean ozone, while colored lines are the contributions to ozone tendency due to horizontal transport (green), vertical transport(red), and chemical production and loss (blue). The sum of all terms in the continuity equation (total tendency) is shown as black dashed line.

examined the tropical O_3 and CO TEM budgets in the WACCM and concluded that the seasonality in vertical transport makes an important contribution to the seasonality of ozone in the tropical lower stratosphere, and horizontal in-mixing is most important at the tropopause level (which is 86 hPa in WACCM). However, they only considered tropical-wide averages of the tracer concentrations and residual velocities. We extend this analysis to consider the budgets in the ST and NT separately, for both WACCM and GEOSCCM simulations.

Figure 6 shows the seasonality of the terms in equation (5) for ST, NT, and tropics-wide ozone at 85 hPa from WACCM and GEOSCCM. In both models there is, consistent with the above analysis, a larger annual cycle in ozone tendency (black curves) in the NT than in the ST. In the ST, the annual cycle in the vertical transport (red curves) is larger than that in the horizontal transport (green curves), and the timing of maximum/minimum in ozone tendency (black line) roughly coincides with the timing of ozone tendency due to vertical transport (red curve), which peaks during the northern winter (most negative) and decreases during the summer. Examination of individual terms in equation (5) indicates that vertical transport is dominated by vertical advection and that eddy mixing dominates the horizontal transport (as found in the tropical average in *Abalos et al.* [2013b]). Thus, consistent with the above analysis, the seasonality in vertical advection plays a major role in driving the seasonality in ST ozone.

The balance in the NT is different from that in the ST. The seasonality in tendency due to horizontal transport is larger than that due to vertical transport, and the tendency due to horizontal transport (mixing) and the total tendency both peak during June–August. This indicates that seasonality in horizontal mixing plays the major role in the NT ozone annual cycle.

While the seasonality of the different terms is similar between WACCM and GEOSCCM, there are some quantitative differences. The ozone seasonality due to vertical transport is larger in WACCM than in GEOSCCM,

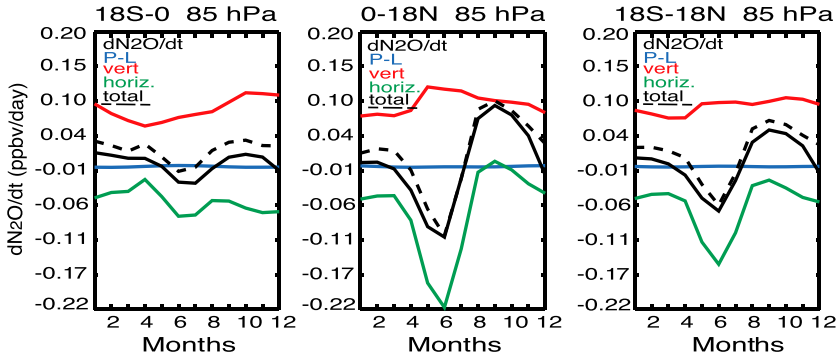

Figure 7. Mean seasonal cycles (monthly means) of terms in the N_2O TEM continuity equation at 85 hPa in GEOSCCM averaged over (left to right) EQ-18°S, EQ-18°N, and 18°S–18°N.

as is the seasonality due to horizontal transport. This is consistent with Figure 4, which shows larger annual amplitude for $\bar{w}^*$ and larger summer to winter ozone gradient in WACCM.

We have focused above on the seasonality in transport, but Figure 6 shows that there is seasonality in chemical production and loss ($P - L$) that is of comparable magnitude to the transport terms, and this seasonality also differs between the NT and ST. In the NT, ozone tendency due to $P-L$ has two minima during solstices and two maxima during equinoxes. In the ST, there are also two minima and maxima in ozone tendency due to $P - L$. However, the ST minimum during the boreal summer (June–August) is larger than during the boreal winter. Furthermore, the summer/winter minimum in the ST is stronger/weaker than that in the NT. The annual cycle in $P-L$ is mainly due to ozone production (photolysis rate), which depends on solar zenith angle and overhead column ozone. The seasonality of solar zenith angle is the same for NT and ST, but overhead column ozone has a stronger seasonal cycle in the NT leading to a small annual cycle in $P - L$.

The described above TEM budget analysis is complicated by the presence of seasonality in photochemical production and loss. This is much less a factor for N_2O where there is no production and very weak loss in the tropical lower stratosphere. Therefore, TEM analysis of N_2O can provide valuable information about the transport and its role in the NT and ST. Figure 7 shows N_2O TEM budgets at 86 hPa in GEOSCCM that look very similar to that shown for ozone with dominant role of vertical transport in the ST and horizontal mixing in the NT. Note that N_2O transport terms (green and red lines) are of opposite signs to those for ozone due to reversed horizontal and vertical gradients.

There is also a good agreement between O_3 and N_2O TEM transport terms above and below 85 hPa (not shown). The seasonal magnitude of transport at 100 hPa in the ST is much smaller than in the NT with peak in upwelling during the winter rather than during the summer. The NT horizontal and vertical transport is of nearly equal amplitude and opposite sign. At higher levels (near 70 hPa) the magnitude of annual cycle due to horizontal transport in the NT is smaller than at 85 hPa, and the NT contribution due to vertical transport is shifted in phase compared to 85 hPa with weaker upwelling during the summer. The N_2O tendencies due to vertical and horizontal transport are then in phase, and the annual cycle in tracers is affected by both upwelling and horizontal mixing.

The TEM analysis of WACCM and GEOSCCM supports the hypothesis that the balance between vertical advection and horizontal mixing differs between the ST and NT lower stratosphere. Agreement in TEM transport terms between O_3 and N_2O provides further evidence that hemispheric differences in the annual cycle amplitude are driven by the transport rather than chemical processes. TEM analysis shows that seasonality of ST O_3 and N_2O is primarily due to seasonality in the upwelling, whereas the strong seasonality of NT ozone is due to a large increase of horizontal mixing during northern summer.

4.2. Longitudinal Variations

Thus far, the analysis has focused on zonal mean tracer concentrations and does not provide any information on longitudinal variations in ozone or the processes causing variations in ozone and other long-lived tracers such as N_2O and HCl. We now examine the zonal variations in ST and NT O_3 in the GEOSCCM and WACCM simulations and MLS-v4 measurements and relate these to variations in mixing and upwelling discussed above.

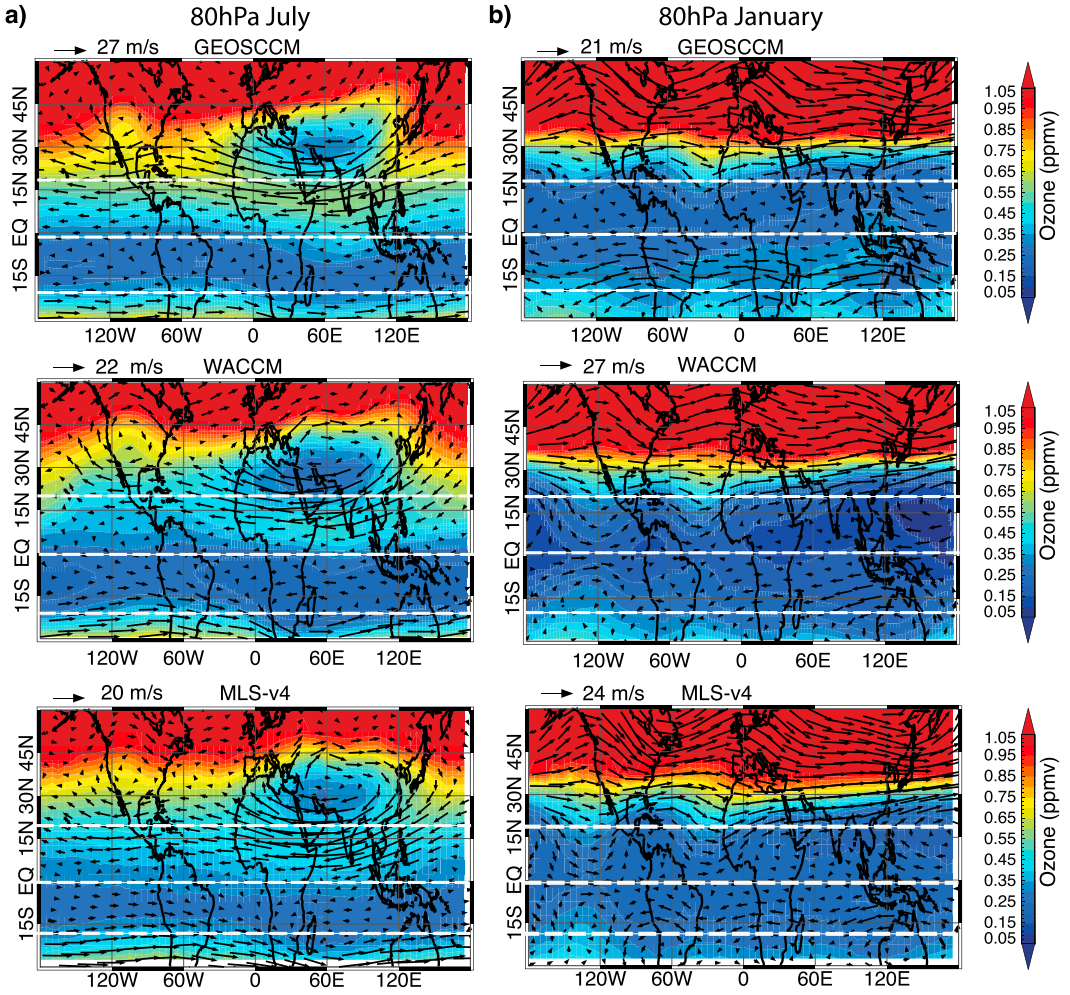

Figure 8. Maps of climatological ozone and horizontal winds (black vectors) in (a) July and (b) January from GEOSCCM (top), WACCM (middle), and MLS-v4/MERRA-2 (bottom). Ozone and horizontal winds from GEOSCCM and WACCM are shown at 80 hPa, while MERRA-2 winds are averaged over 70 and 100 hPa pressure levels and plotted over 82.5 hPa ozone from MLS. Dashed white lines indicate the boundaries of the northern (0–20°N) and southern (0–20°S) tropics. Ozone values larger than 1.05 ppmv are shaded in dark red.

We first examine the maps of climatological monthly-mean 80 hPa ozone mixing ratios and horizontal winds for July and January (Figure 8). These correspond to the months when the NT-averaged ozone is at its maximum and minimum values, respectively (the ST ozone maximum and minimum occur 1–2 months later). During July, the most distinct nonzonal feature is a region of low ozone centered around 30°N over the Indian subcontinent. Southeast of this, there is a band of higher ozone that penetrates from the extratropical Pacific into the NT (around 60°E). As discussed in previous studies and also shown in Figure 8 by wind vectors from GEOSCCM and WACCM simulations, the low ozone over the Indian subcontinent and mixing of high ozone into the tropics are connected to the Asian American monsoon anticyclone. [e.g., *Konopka et al.*, 2010; *Randel and Park*, 2006; *Park et al.*, 2007]. There is also transport of ozone rich air to the tropics above North America, identified as weaker than above the Asia anticyclonic circulation (North American monsoon anticyclone). The penetration of ozone rich air by the Asian monsoon anticyclone is larger in GEOSCCM compared to MLS and WACCM and reaches across the equator into the ST.

The strength of these features varies with height. There is lower ozone over the Indian subcontinent and stronger penetration of high ozone into the tropics at 100 hPa in MLS and both simulations, whereas the features are weaker at 70 hPa (not shown). As the influence of monsoons and other disturbances of the tropospheric origin decreases at higher altitudes, so do the zonal differences in ozone seasonal cycle. This is

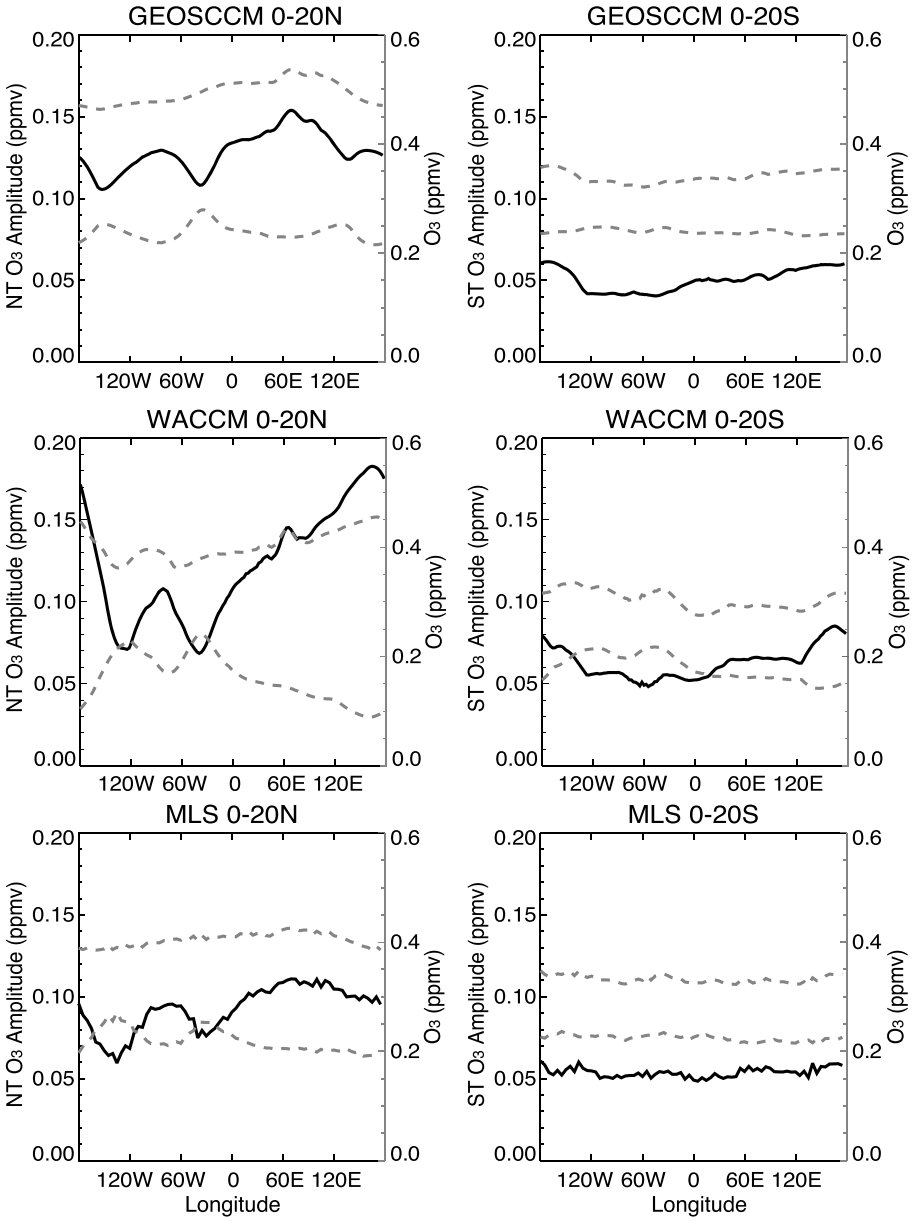

Figure 9. Zonal variations in the (left column) NT and (right column) ST annual cycle magnitude (solid black curve) and in maximum (upper dashed gray curve) and minimum (lower dashed gray curve) ozone mixing ratio during the climatological year from (top) GEOSCCM, (middle) WACCM, and (bottom) MLS.

consistent with TEM analysis and the results for the tropical mean balance in *Abalos et al.* [2013b] that showed the decrease with height in the seasonality of ozone tendency due to horizontal mixing.

Monsoon-generated nonzonal features described above are also found in other trace gases, such as HCl, N_2O, and CO (not shown). This suggests a large impact of eddy mixing on the tracer seasonality in NT. The strength of in-mixing and its relative role, however, vary among the tracers and strongly depend on the lower stratospheric latitudinal gradient of the considered tracer [*Ploeger et al.*, 2012]. For example, water vapor is almost unaffected by the horizontal transport near the tropical tropopause due to the very weak difference in mixing ratios between tropical and extratropical regions.

In January (Figure 8b), there are lower mixing ratios and weaker latitudinal gradients in the tropical ozone than in July for both NT and ST. Furthermore, the zonal variations are also weaker. There are regions of slightly lower equatorial ozone above the central Pacific Ocean (near 170°E) and the continents of South America

and Africa (regions of enhanced deep convection). These smaller ozone values coincide with anticyclone circulation within the NT, which isolates the air inside the regions of the anticyclones. There is also penetration of higher ozone into the NT over the eastern Pacific (120°W) and Atlantic (30°W) oceans. Low ozone is likely connected with tropical upwelling over regions of tropical convection, while penetration of high ozone over ocean could be connected with subtropical wave breaking. The strong subtropical jet in winter acts as a barrier for horizontal transport except over the Pacific and Atlantic Oceans where Rossby wave breaking is common [*Waugh and Polvani*, 2000], resulting in high ozone being mixed into the tropics. The differences between the models and observations could be linked to differences in the jet structure and/or in the Rossby waves.

The zonal variations in January and July NT ozone have the potential to cause zonal variations in the annual amplitude. To examine this, we plot in Figure 9 the longitudinal variations in the amplitude of the annual cycle (solid curve) together with the variations in the annual minimum (lower dashed) and maximum (upper dashed) values for ozone at 80 hPa from GEOSCCM, WACCM, and MLS. As discussed above, the NT seasonal maximum roughly corresponds to the boreal summer and minimum to the boreal winter, while the ST seasonal maximum and minimum are 1–2 months later than in the NT. There are small zonal variations in the annual amplitude in ST ozone (especially in MLS and GEOSCCM), consistent with small zonal variations in ST in Figure 8. There are, however, substantial variations in the NT, with the largest annual amplitude occurring around 90–120°E and a secondary maximum around 80°W. There are differences in the magnitude of zonal variations and locations of the peaks between the models and between models and observations, but the same qualitative variation occurs in all three. The maximum around 90–120°E is due primarily to an increase in the NT ozone during annual maximum within this longitude range and is associated with mixing-in of midlatitude ozone into the NT due to the Asian summer monsoon anticyclone discussed above (Figure 8a). In contrast, the local maximum in the amplitude around 80°W is primarily due to variations in the annual minimum, with larger annual-minimum ozone around 30°W and 150°W. These variations are due to the penetration of higher ozone in NT over the Atlantic and eastern Pacific Oceans during NH winter (see above, Figure 8b). This wintertime penetration of ozone is stronger in WACCM than in GEOSCCM or MLS.

In summary, the amplitude of the seasonal cycle in ozone varies with longitude, and these variations are due to increased eddy mixing around 90–120°E during summer associated with the Asian monsoon and increased mixing over the Pacific and Atlantic during NH winter. The signal of wintertime mixing is only seen in WACCM TEM analysis in Figure 6 as a small increase in ozone tendency due to horizontal transport during winter months (most likely due to stronger wintertime penetration of ozone over the Atlantic and eastern Pacific Oceans in WACCM than in GEOSCCM).

5. Conclusions

Stolarski et al. [2014] showed that there is a hemispheric difference in the annual cycle of tropical lower stratospheric ozone, with larger amplitude in the northern tropics (NT) than in the southern tropics (ST). In this study, we have examined the ability of CCM simulations from CCMVal-2 to reproduce this hemispheric difference and used two of the CCMs to examine the cause. Testing whether CCMs produce the correct spatial structure of tracers' annual cycle is a valuable tool for evaluating the models' performance in the tropical lower stratosphere, as it indicates the correct balance between transport and chemical processes.

Examination of the CCM simulations showed a large variability in the annual cycle of tropical lower stratospheric O_3. The majority of the CCMs produced the observed feature of a larger annual cycle in the NT than ST, but there are several with similar amplitude in the ST and NT or even with a larger amplitude in the ST. Further, even for models with larger amplitudes in the NT there was a large range in size, with several models showing unrealistically small or large amplitudes. As a result, only around a third of the models produce an ozone annual cycle similar to that observed. A similar analysis of the NT-averaged and ST-averaged amplitude of annual cycle in other long-lived tracers (N_2O, HCl, and mean age) shows very similar results, suggesting that the NT-ST contrast in annual amplitude is driven by transport and not chemistry. This indicates that the majority (two thirds) of the CCMs have problems in representing transport in the tropical lower stratosphere, which is broadly consistent with previous studies of transport in CCMVal-2 models [e.g., *Strahan et al.*, 2011].

Analysis of the relationship between the vertical transport by the residual circulation and ozone among CCMs provided insights to the cause of the hemispheric differences in the ozone annual cycle. For the ST, the spread in the simulated amplitude of the annual cycle in vertical transport explains most of the spread in the simulated amplitude of the ozone annual cycle, i.e., CCMs with larger annual cycle in ST upwelling tend to have

a large annual cycle in ST ozone. In contrast, there is no relationship between the amplitudes of the annual cycle of vertical advection and O_3 for the NT. This indicates that seasonality in upwelling is a major driver of seasonality of ozone in the ST, but other processes (presumably mixing) must be dominating in the NT.

A TEM analysis of WACCM and GEOSCCM simulations provided additional insights to the cause of the hemispheric differences in the annual cycle of ozone and other tracers. We confirmed the importance of seasonality in vertical advection in causing the seasonality in the ST and showed that seasonality of horizontal mixing drives the seasonality in NT O_3 and N_2O. The seasonality of ozone is also influenced by the seasonality of photochemical sources and sinks, which differ between NT and ST, but local chemistry does not play a role in ST-NT contrast in N_2O. As discussed in previous studies [*Konopka et al.*, 2010; *Randel and Park*, 2006; *Park et al.*, 2007], enhanced horizontal mixing during boreal summer is primarily associated with the Asian monsoon anticyclone causing an increase in NT ozone (and a decrease in NT N_2O).

There are several outstanding issues from this study. One is the causes of the differences between annual cycles from the different ozone data sets, which data set is most realistic. Of particular importance is whether the double peak structure in the vertical is real or an artifact of the sampling, resolution, or uncertainties of the data. Clarification of this issue is needed for a more detailed analysis of the tropical transport and evaluation of the CCMs (especially as none of the models shows the double peak structure).

Similarly, the cause of the spread in ozone annual cycle among the CCMs needs further examination. A process-based analysis, such as the TEM analysis, would be useful if applied to all of the individual models. The CCM simulations examined here are generally not from the latest versions of the CCMs, and it will be of value to repeat this analysis using simulations submitted to the new SPARC/IGAC CCM Initiative [*Eyring et al.*, 2013] and to also compare with other transport diagnostics (such as those considered in *Strahan et al.*, 2011).

Acknowledgments
This material is based upon work supported by the National Science Foundation Graduate Research Fellowship Program under grant (DGE-1232825). We thank the NASA MAP program for supporting the GEOSCCM simulations and the NASA Center for Climate Simulation (NCCS) for providing the high-performance computing resources. We acknowledge the Chemistry-Climate Model Validation (CCMVal) Activity for WCRP's (World Climate Research Programme) SPARC (Stratospheric Processes and their Role in Climate) project for organizing and coordinating the model data analysis activity, and the British Atmospheric Data Centre (BADC) for collecting and archiving the CCMVal model output. We would also like to acknowledge, and thank, William Seviour for providing us with w*, calculated from ERA-Interim reanalysis product and all those who are members of the modeling and data science and support teams. Readers can find and access the data used in this study in the cited references, table, and at provided in "the Observational Data" section URLs. We thank the three reviewers for their substantive comments, which helped to improve the manuscript.

References

Abalos, M., W. Randel, and E. Serrano (2012), Variability in upwelling across the tropical tropopause and correlations with tracers in the lower stratosphere, *Atmos. Chem. Phys.*, *12*(23), 11,505–11,517.

Abalos, M., F. Ploeger, P. Konopka, W. Randel, and E. Serrano (2013a), Ozone seasonality above the tropical tropopause: Reconciling the Eulerian and Lagrangian perspectives of transport processes, *Atmos. Chem. Phys.*, *13*(21), 10,787–10,794.

Abalos, M., W. Randel, D. Kinnison, and E. Serrano (2013b), Quantifying tracer transport in the tropical lower stratosphere using WACCM, *Atmos. Chem. Phys.*, *13*(10), 591–510.

Akiyoshi, H., L. Zhou, Y. Yamashita, K. Sakamoto, M. Yoshiki, T. Nagashima, M. Takahashi, J. Kurokawa, M. Takigawa, and T. Imamura (2009), A CCM simulation of the breakup of the Antarctic polar vortex in the years 1980–2004 under the CCMVal scenarios, *J. Geophys. Res.*, *114*, D03103, doi:10.1029/2007JD009261.

Andrews, D. G., J. R. Holton, and C. B. Leovy (1987), *Middle Atmosphere Dynamics*, vol. 40, Academic Press, New York.

Austin, J., and N. Butchart (2003), Coupled chemistry climate model simulations for the period 1980 to 2020: Ozone depletion and the start of ozone recovery, *Q. J. R. Meteorol. Soc.*, *129*(595), 3225–3249.

Austin, J., and R. J. Wilson (2006), Ensemble simulations of the decline and recovery of stratospheric ozone, *J. Geophys. Res.*, *111*, D16314, doi:10.1029/2005JD006907.

Douglass, A., R. Stolarski, S. Strahan, and L. Oman (2012), Understanding differences in upper stratospheric ozone response to changes in chlorine and temperature as computed using CCMVal-2 models, *J. Geophys. Res.*, *117*, D16306, doi:10.1029/2012JD017483.

Déqué, M. (2007), Frequency of precipitation and temperature extremes over France in an anthropogenic scenario: Model results and statistical correction according to observed values, *Global Planet. Change*, *57*(1), 16–26.

Eyring, V., M. P. Chipperfield, M. A. Giorgetta, D. E. Kinnison, E. Manzini, K. Matthes, P. A. Newman, S. Pawson, T. G. Shepherd, and D. W. Waugh, (2008), Overview of the new CCMVal reference and sensitivity simulations in support of upcoming ozone and climate assessments and the planned SPARC CCMVal report, SPARC Newsl. No. 30, pp. 20–26, WMO-WRCP, Geneva, Switz.

Eyring, V., et al. (2013), Overview of IGAC/SPARC Chemistry-Climate Model Initiative (CCMI) community simulations in support of upcoming ozone and climate assessments, SPARC Newsl. No. 40, pp. 48–66, WMO-WRCP, Geneva, Switzerland.

Fueglistaler, S., A. Dessler, T. Dunkerton, I. Folkins, Q. Fu, and P. W. Mote (2009), Tropical tropopause layer, *Rev. Geophys.*, *47*, RG1004, doi:10.1029/2008RG000267.

Garcia, R., D. Marsh, D. Kinnison, B. Boville, and F. Sassi (2007), Simulation of secular trends in the middle atmosphere, 1950–2003, *J. Geophys. Res.*, *112*, D09301, doi:10.1029/2006JD007485.

Garny, H., M. Dameris, and A. Stenke (2009), Impact of prescribed SSTs on climatologies and long-term trends in CCM simulations, *Atmos. Chem. Phys.*, *9*(16), 6017–6031.

Haynes, P., and E. Shuckburgh (2000), Effective diffusivity as a diagnostic of atmospheric transport: 1. Stratosphere, *J. Geophys. Res.*, *105*(22), 777–722.

Jourdain, L., S. Bekki, F. Lott, and F. Lefévre (2008), The coupled chemistry-climate model LMDz-REPROBUS: Description and evaluation of a transient simulation of the period 1980–1999, *Ann. Geophys.*, *26*, 1391–1413. Copernicus GmbH.

Jöckel, P., et al. (2006), The atmospheric chemistry general circulation model ECHAM5/MESSy1: Consistent simulation of ozone from the surface to the mesosphere, *Atmos. Chem. Phys. Discuss.*, *6*(4), 6957–7050.

Konopka, P., J. Grooß, F. Ploeger, and R. Müller (2009), Annual cycle of horizontal in-mixing into the lower tropical stratosphere, *J. Geophys. Res.*, *114*, D19111, doi:10.1029/2009JD011955.

Konopka, P., J.-U. Grooß, G. Günther, F. Ploeger, R. Pommrich, R. Müller, and N. Livesey (2010), Annual cycle of ozone at and above the tropical tropopause: Observations versus simulations with the Chemical Lagrangian Model of the Stratosphere (CLaMS), *Atmos. Chem. Phys.*, *10*(1), 121–132.

Kramarova, N., E. Nash, P. Newman, P. Bhartia, R. McPeters, D. Rault, C. Seftor, P. Xu, and G. Labow (2014), Measuring the Antarctic ozone hole with the new Ozone Mapping and Profiler Suite (OMPS), *Atmos. Chem. Phys.*, *14*(5), 2353–2361.

Lamarque, J., D. Kinnison, P. Hess, and F. Vitt (2008), Simulated lower stratospheric trends between 1970 and 2005: Identifying the role of climate and composition changes, *J. Geophys. Res.*, *113*, D12301, doi:10.1029/2007JD009277.

Livesey, N., et al. (2008), Validation of Aura Microwave Limb Sounder O_3 and CO observations in the upper troposphere and lower stratosphere, *J. Geophys. Res.*, *113*, D15S02, doi:10.1029/2007JD008805.

Livesey, N. J., et al. (2015), Version 4.2x level 2 data quality and description document, *Tech. Rep. JPL d-33509 Rev. B*Jet Propul. Lab., California Institute of Technology, Pasadena, Calif. [Available at http://mls.jpl.nasa.gov.]

Ming, A., P. Hitchcock, and P. Haynes (2016a), The response of the lower stratosphere to zonally symmetric thermal and mechanical forcing, *J. Atmos. Sci.*, *73*(5), 1903–1922.

Ming, A., A. C. Maycock, P. Hitchcock, and P. Haynes (2016b), *The Radiative Role of Ozone and Water Vapour in the Annual Temperature Cycle in the Tropical Tropopause Layer*, vol. 17, pp. 5677–5701.

Morgenstern, O., P. Braesicke, F. O'Connor, A. Bushell, C. Johnson, S. Osprey, and J. Pyle (2009), Evaluation of the new UKCA climate-composition model—Part 1: The stratosphere, *Geosci. Model Dev.*, *2*(1), 43–57.

Morgenstern, O., et al. (2010), Review of the formulation of present-generation stratospheric chemistry-climate models and associated external forcings, *J. Geophys. Res.*, *115*, D00M02, doi:10.1029/2009JD013728.

Oman, L. D., and A. R. Douglass (2014), Improvements in total column ozone in GEOSCCM and comparisons with a new ozone-depleting substances scenario, *J. Geophys. Res. Atmos.*, *119*, 5613–5624, doi:10.1002/2014JD021590.

Park, M., W. J. Randel, A. Gettelman, S. T. Massie, and J. H. Jiang (2007), Transport above the Asian summer monsoon anticyclone inferred from Aura Microwave Limb Sounder tracers, *J. Geophys. Res.*, *112*, D16309, doi:10.1029/2006JD008294.

Pawson, S., R. S. Stolarski, A. R. Douglass, P. A. Newman, J. E. Nielsen, S. M. Frith, and M. L. Gupta (2008), Goddard Earth observing system chemistry-climate model simulations of stratospheric ozone-temperature coupling between 1950 and 2005, *J. Geophys. Res.*, *113*, D12103, doi:10.1029/2007JD009511.

Pitari, G., E. Mancini, V. Rizi, and D. Shindell (2002), Impact of future climate and emission changes on stratospheric aerosols and ozone, *J. Atmos. Sci.*, *59*(3), 414–440.

Ploeger, F., P. Konopka, R. Müller, S. Fueglistaler, T. Schmidt, J. Manners, J. Grooß, G. Günther, P. Forster, and M. Riese (2012), Horizontal transport affecting trace gas seasonality in the Tropical Tropopause Layer (TTL), *J. Geophys. Res.*, *117*, D09303, doi:10.1029/2011JD017267.

Randel, W. J., and M. Park (2006), Deep convective influence on the Asian summer monsoon anticyclone and associated tracer variability observed with Atmospheric Infrared Sounder (AIRS), *J. Geophys. Res.*, *111*, D12314, doi:10.1029/2005JD006490.

Randel, W. J., M. Park, F. Wu, and N. Livesey (2007), A large annual cycle in ozone above the tropical tropopause linked to the Brewer-Dobson circulation, *J. Atmos. Sci.*, *64*(12), 4479–4488.

Riese, M., F. Ploeger, A. Rap, B. Vogel, P. Konopka, M. Dameris, and P. Forster (2012), Impact of uncertainties in atmospheric mixing on simulated UTLS composition and related radiative effects, *J. Geophys. Res.*, *117*, D16305, doi:10.1029/2012JD017751.

Schraner, M., et al. (2008), Technical note: Chemistry-climate model SOCOL: Version 2.0 with improved transport and chemistry/microphysics schemes, *Atmos. Chem. Phys.*, *8*(19), 5957–5974.

Scinocca, J., N. McFarlane, M. Lazare, J. Li, and D. Plummer (2008), Technical Note: The CCCma third generation AGCM and its extension into the middle atmosphere, *Atmos. Chem. Phys.*, *8*(23), 7055–7074.

Shibata, K., and M. Deushi (2008), Long-term variations and trends in the simulation of the middle atmosphere 1980-2004 by the chemistry-climate model of the Meteorological Research Institute, *Ann. Geophys.*, *26*, 1299–1326. Copernicus GmbH.

SPARC CCMVal (2010), *SPARC Report on the Evaluation of Chemistry-Climate Models*, edited by V. Eyring, T. G. Shepherd, and D. W. Waugh, SPARC IPO, Toronto, Canada.

Stolarski, R. S., D. W. Waugh, L. Wang, L. D. Oman, A. R. Douglass, and P. A. Newman (2014), Seasonal variation of ozone in the tropical lower stratosphere: Southern tropics are different from northern tropics, *J. Geophys. Res. Atmos.*, *119*, 6196–6206, doi:10.1002/2013JD021294.

Strahan, S. E., et al. (2011), Using transport diagnostics to understand chemistry climate model ozone simulations, *J. Geophys. Res.*, *116*, D17302, doi:10.1029/2010JD015360.

Teyssédre, H., et al. (2007), A new tropospheric and stratospheric Chemistry and Transport Model MOCAGE-Climate for multi-year studies: Evaluation of the present-day climatology and sensitivity to surface processes, *Atmos. Chem. Phys.*, *7*(22), 5815–5860.

Tian, W., and M. P. Chipperfield (2005), A new coupled chemistry-climate model for the stratosphere: The importance of coupling for future O_3-climate predictions, *Q. J. R. Meteorol. Soc.*, *131*(605), 281–303.

Wang, H. J., D. M. Cunnold, L. W. Thomason, J. M. Zawodny, and G. E. Bodeker (2002), Assessment of SAGE version 6.1 ozone data quality, *J. Geophys. Res.*, *107*(D23), 4691, doi:10.1029/2002JD002418.

Waugh, D. W., and L. M. Polvani (2000), Climatology of intrusions into the tropical upper troposphere, *Geophys. Res. Lett.*, *27*(23), 3857–3860.